Rapid Communications

Noise correlations in time- and angle-resolved photoemission spectroscopy

Christopher Stahl and Martin Eckstein
Department of Physics, University of Erlangen-Nuremberg, Staudtstraße 7, 91058 Erlangen, Germany

(Received 24 December 2018; published 20 June 2019)

In time-resolved photoemission experiments, more than one electron can be emitted from the solid by a single ultrashort pulse. We theoretically demonstrate how correlations between the momenta of outgoing electrons relate to time-dependent two-particle correlations in the solid. This can extend the scope of time- and angle-resolved photoemission spectroscopy to probe superconducting and charge density fluctuations in systems without long-range order, and to reveal their dynamics independent of the electronic gap and thus unrestricted by the energy-time uncertainty. The proposal is illustrated for superconductivity in a BCS model. An impulsive perturbation can quench the gap on ultrafast timescales, while nonequilibrium pairing correlations persist much longer, even when electron-electron scattering beyond mean-field theory is taken into account. There is thus a clear distinction between a dephasing of the Cooper pairs and the thermalization into the normal state. While a measurement of the gap would be blind to such pairing correlations, they can be revealed by the angular correlations in photoemission.

DOI: 10.1103/PhysRevB.99.241111

Angle-resolved photoemission spectroscopy (ARPES) is a powerful technique to probe the electronic structure in solids. With short laser pulses in a pump-probe setup one can moreover achieve femtosecond time resolution, which has opened a unique path to explore the light-induced dynamics of collective phases in solids on ultrashort timescales [1]. Time-resolved ARPES (tr-ARPES) has been used to study ultrafast quasiparticle dynamics [2,3], laser manipulation of electronic orders [4–6], photoinduced Mott metal-insulator transitions [7–9], and Floquet Bloch bands [10]. An intriguing aim of the ultrafast manipulation of condensed matter phases is to control orders such as magnetism, charge-density waves, or superconductivity. Although the corresponding order parameters are revealed in the electronic spectra, e.g., through the opening of a gap, some fundamental challenges remain to probe their dynamics using ARPES: (i) Spectroscopic probes are limited by the energy-time uncertainty, while the relevant dynamical processes in the destruction or formation of an order parameter ϕ (such as the superconducting condensate density) may be faster than the inverse of the gap Δ which identifies ϕ in the electronic spectrum [11] or happen on the same scale, as for the amplitude mode in superconductors [12–16]. (ii) Collective orders can exhibit strong fluctuations on the nanoscopic scale without forming a long-range order, and furthermore, the nonequilibrium dynamics of such fluctuations can proceed entirely different from the single-particle dynamics. For example, fluctuations of the atomic positions at a light-induced lattice change evolve nontrivially different from the mean [17], and one can distinguish ultrafast demagnetization via a reduction of the exchange splitting (which is reflected in the single-particle bands) versus a dephasing of spin waves [18]. Recent theoretical proposals regard light-induced (critical) dynamics of pairing or antiferromagnetic fluctuations [19–21], or nonthermal dynamics of stripe order in cuprates [22]. A measurement of fluctuations of electronic orders is thus indispensable for the understanding of the dynamics in complex materials.

Modern time-of-flight detectors for ARPES image outgoing electrons with different momenta onto different pixels of a detector, and thus allow one to simultaneously record two electrons which are emitted from a single ultrashort probe pulse into different angular directions. In this Rapid Communication, we propose that information on time-dependent two-particle correlations in the solid can be revealed from the correlation between the emission into different directions, i.e., the shot-to-shot noise correlation on the detector. The intriguing potential in measuring noise has been demonstrated in various other settings. For example, noise correlation in time-of-flight measurements of the momentum distribution in ultracold gases [23,24] can distinguish different phases of the initially trapped quantum state, and the shot-to-shot variance of the reflectivity in optical pump-probe experiments has been used to detect squeezing of vibrational modes in a quartz crystal [25], and to measure the current noise in photoexcited bismuth to probe nonthermal electrons [26].

Two-particle correlations in photoemission have been used previously to study electronic interactions in equilibrium [27–29]. The process discussed here is an emission of two electrons by two photons from the same ultrashort pulse (different from a double photoemission where one photon leads to the emission of two electrons due to secondary processes, and different from two-photon photoemission, where one electron is emitted by the absorption of two photons [30–32]), and thus allows a theoretical interpretation along the same lines as the conventional theory for time-resolved photoemission spectroscopy [33–35]. We start from a Hamiltonian $H = H_s + H_e + H'$, where H_s is the Hamiltonian of the solid, and $H_e = \sum_{p\sigma} E_p f^\dagger_{p\sigma} f_{p\sigma}$ describes the emitted electrons with asymptotic momentum p and spin σ ($E_p = p^2/2m + W$, with the work function W). The Hamiltonian H_s can be time dependent to incorporate a nonperturbative excitation,

 ©2019 American Physical Society

which also determines a well-defined time zero $t = 0$. The excitation could be a pump pulse centered around $t = 0$, or any other protocol which creates an excited state at $t = 0$. (Pump pulses which overlap with the probe could be included along the same lines, as long as photoemission due to the pump is neglected. For simplicity, we restrict the discussion to nonoverlapping pump and probe, such that the momentum of the outgoing states is a gauge-invariant observable [35].) Electron emission is due to the coupling term

$$H' = \sum_{k,p,\sigma,\sigma'} S(t)^* e^{i\Omega t} M_{k,p}^{\sigma,\sigma'} f_{p\sigma'}^\dagger c_{k\sigma} + \text{H.c.}, \tag{1}$$

where $M_{k,p}^{\sigma,\sigma'} \equiv \delta_{\sigma,\sigma'} M_{k,p}$ are matrix elements (for notational simplicity we restrict the solid to one band with electron operators $c_{k\sigma}$), and $S(t)$ is the temporal envelope of the probe with frequency Ω centered around $t > 0$ after the excitation. The Hamiltonian H has built in two basic assumptions which are commonly made in the theory of ARPES: (i) There is no interaction between electrons in outgoing states (f_p) and electrons in the solid (c_k), manifesting the sudden approximation. Furthermore, (ii), we neglect interactions between outgoing electron and space-charge effects, which is controlled by the excitation density. Finally, all illustrating calculations below are based on simple matrix elements $M_{k,p} = M\delta_{k,p}$. This corresponds to full momentum conservation, as in two-dimensional materials where only the momentum parallel to the surface matters. Matrix element effects could easily be reinstated for an interpretation of real experiments.

A time-resolved ARPES measurement records the total population $I_{p\sigma}^{(1)} = \langle n_{p\sigma}^f \rangle_{t=\infty}$ in an outgoing state ($n_{p\sigma}^f = f_{p\sigma}^\dagger f_{p\sigma}$), which is accumulated over the entire probe pulse duration (until $t = \infty$). Because two electrons can be emitted by two photons from the same pulse, we can measure the correlations $\Delta I_{p\sigma,p'\sigma'} = I_{p\sigma,p'\sigma'}^{(2)} - I_{p\sigma}^{(1)} I_{p'\sigma'}^{(1)}$ at $p \neq p'$, with $I_{p\sigma,p'\sigma'}^{(2)} = \langle n_{p\sigma}^f n_{p'\sigma'}^f \rangle_{t=\infty}$, corresponding to the statistical correlations of photoemission events from a number of probe pulses. Note that the response time of the detector only has to be fast enough to distinguish the events from separate probe pulses (which is possible by today's detectors), but not the arrival time difference of photoelectrons from the same pulse. For a weak probe pulse, all signals are obtained using the leading-order time-dependent perturbation theory in the coupling H', which is second order for $I^{(1)}$ and fourth order for $I^{(2)}$. We assume that at $t = -\infty$ the outgoing states are empty, and the solid is described by its initial density matrix ρ_0^s. Switching to interaction representation in H' yields $I_{p\sigma,p'\sigma'}^{(2)} = \langle \mathcal{S}^\dagger n_{p\sigma}^f n_{p'\sigma'}^f \mathcal{S} \rangle_0$, where $\mathcal{S} = T_t e^{-i\int_{-\infty}^{+\infty} d\bar{t} H'(\bar{t})}$ is the S matrix, and $\langle \cdots \rangle_0$ the initial-state expectation value. Because the initial state does not contain outgoing electrons, the leading-order expansion of $\mathcal{S}$ and $\mathcal{S}^\dagger$ in terms of H' is second order and must contain both $f_{p\sigma}^\dagger$ and $f_{p'\sigma'}^\dagger$ (both $f_{p\sigma}$ and $f_{p'\sigma'}$) in $\mathcal{S}$ ($\mathcal{S}^\dagger$), respectively. After the expansion, the expectation value factorizes for the solid and the outgoing states, so that the result can be expressed in terms of one- and two-point Green's functions of the solid, $G(1, 1') = \langle c(1)^\dagger c(1') \rangle_0$ and

$$G(1, 2, 2', 1') = \langle T_{\bar{t}}[c(1)^\dagger c(2)^\dagger] T_t[c(2')c(1')] \rangle_0. \tag{2}$$

Here, $1 \equiv (k_1, \sigma_1, t_1)$, etc., is short for space-time variables, and T_t ($T_{\bar{t}}$) is the (anti)-time ordering operator for fermions. Finally all terms can be combined to [36]

$$I_{p\sigma}^{(1)} = \int d1 d1' M_{1,1'}^{p,\sigma} G(1, 1'), \tag{3}$$

$$I_{p\sigma,p'\sigma'}^{(2)} = \int d1 d1' d2 d2' M_{1,1'}^{p,\sigma} M_{2,2'}^{p',\sigma'} G(1, 2, 2', 1'), \tag{4}$$

where $\int d1 = \sum_{k_1,\sigma_1} \int_{-\infty}^{\infty} dt_1$, and

$$M_{1,1'}^{p,\sigma} = M_{k_1,p}^{\sigma_1,\sigma} \left(M_{k_1',p}^{\sigma_1',\sigma}\right)^* S(t_1) S(t_1')^* e^{i(E_p - \Omega)(t_1 - t_1')}. \tag{5}$$

The expression for $I_{p\sigma}^{(1)}$ is the conventional expression for time-resolved ARPES [33,34], which can be understood as a time-dependent filter $M(t, t')$ applied to the single-particle propagator [37]. Equation (4) provides an analogous view on two-particle quantities.

To illustrate the use of noise correlation in time-resolved ARPES, one can consider an ideal ultrashort pulse $S(t) = A\delta(t - t_0)$. In this case, Eqs. (3) and (4) yield $I_{p\sigma}^{(1)} = |AM|^2 \langle n_{p\sigma}^c \rangle_{t=t_0}$ and

$$\Delta I_{p\sigma,p'\sigma'}^{(2)} = |AM|^4 \left(\langle n_{p\sigma}^c n_{p'\sigma'}^c \rangle - \langle n_{p\sigma}^c \rangle \langle n_{p'\sigma'}^c \rangle \right)_{t=t_0}, \tag{6}$$

where $n_{p\sigma}^c = c_{p\sigma}^\dagger c_{p\sigma}$ is the momentum occupation, and $\langle O \rangle_t$ is the expectation value of an operator *in the solid* at time t. The angular correlations thus directly yield the momentum correlations in the solid, which can provide unique information on the state. In the BCS wave function, e.g., $\langle n_{k\uparrow}^c n_{-k\downarrow}^c \rangle - \langle n_{k\uparrow}^c \rangle \langle n_{-k\downarrow}^c \rangle = |\langle c_{k\uparrow} c_{-k\downarrow} \rangle|^2$ is a direct measure of pairing correlations, while $\langle n_{k\sigma}^c \rangle$ remains smooth throughout the superconducting transition.

By looking at different pairs k, k' ($k \neq k'$) in $\Delta I_{k,k'}$, different symmetry broken phases can be characterized (charge-density waves, superconductivity, etc.). In the following we provide an illustrative example for using the noise correlations in the study of superconductivity. We start the discussion from the Hubbard model

$$H = -J \sum_{\langle i,j \rangle,\sigma} c_{i\sigma}^\dagger c_{j\sigma} + U/2 \sum_{i,\sigma} n_{i\sigma} n_{i-\sigma}, \tag{7}$$

which is the paradigmatic Hamiltonian to describe the physics of interacting electrons. Here, J is a hopping between nearest-neighbor sites on a lattice, and U is an on-site interaction. We choose an attractive interaction $U < 0$, which leads to s-wave superconductivity. To understand the rich nonequilibrium dynamics in superconductors, it is illustrative to recapitulate first the time-dependent mean-field solution. By decoupling the interaction term in the Cooper channel, the BCS Hamiltonian $H_{\text{BCS}} = \sum_k \hat{\psi}_k^\dagger \hat{h}_k \hat{\psi}_k$ is obtained. Here, $\hat{\psi}_k = (c_{k\uparrow}, c_{-k\downarrow}^\dagger)^T$ is the Nambu spinor and $\hat{h}_k = \hat{\sigma}_z \epsilon_k + \hat{\sigma}_x \Delta' - \hat{\sigma}_y \Delta''$, with the electron dispersion ϵ_k and the gap $\Delta = \Delta' + i\Delta'' = U \sum_k \langle c_{-k\downarrow} c_{k\uparrow} \rangle$. The BCS Hamiltonian can be written in terms of the Anderson pseudospins $\vec{s}_k = \frac{1}{2} \hat{\psi}_k^\dagger \vec{\sigma} \hat{\psi}_k$ [38], which follow the equation of motion $\dot{\vec{s}}_k = \vec{B}_k \times \vec{s}_k$ with the pseudomagnetic field $\vec{B}_k = (2\Delta', -2\Delta'', 2\epsilon_k)$. This defines an integrable set of coupled linear differential equations with an infinite number of conserved quantities [13,39,40]. A simple protocol such as a sudden quench or ramp of the interaction

can lead to collective amplitude modes or an ultrafast vanishing of the gap [12,13]. It must be emphasized that the mean-field dynamics is highly nonthermal, even after a melting of the gap. For example, after a quench of the interaction to $U = 0$ in H_{BCS}, the gap exponentially decays as $\Delta(t) \sim e^{-2t\Delta(0)}$, while the Cooper-pair correlations $F_k = |\langle c_{-k\downarrow} c_{k\uparrow}\rangle|$ at each k remain nonzero, because the Anderson pseudospins $\vec{s}_k$ simply precess at different frequencies, such that the global order only dephases [39]. In contrast, thermalization to a normal state above T_c (e.g., due to electron-electron scattering) would imply $F_k = 0$.

In the following we demonstrate that thermalization and dephasing of superconducting order can be distinct even when realistic electron-electron scattering beyond mean-field theory is taken into account, and that the noise correlations provide a unique measure to distinguish them experimentally. We examine a simple quench or ramp of the interaction, which initiates dynamics representative for a generic impulsive excitation: The final value of U determines the electron-electron scattering and the pairing interaction during the dynamics, while the quench or ramp amplitude mainly sets the excitation density. To incorporate electron-electron scattering beyond mean-field theory, the Hubbard model is solved using nonequilibrium dynamical mean-field theory (DMFT) and an impurity solver based on iterated perturbation theory [41]. We use a semielliptic density of states $D(\epsilon)$, where the half bandwidth $W = 2$ sets the unit of energy and time ($\hbar = 1$). DMFT gives access to all normal and anomalous single-particle Green's function in the lattice, in particular the condensate density $\phi = \sum_k \langle c_{-k\downarrow} c_{k\uparrow}\rangle$ and the individual F_k. Momentum-dependent quantities g_k are represented as functions of the band energy $\epsilon_k \in (-2, 2)$ (Fermi energy $\epsilon_F = 0$), and momentum averages are given by the integral $\sum_k g_k \equiv \int d\epsilon D(\epsilon) g(\epsilon)$.

Figure 1(a) shows the order parameter $\phi(t)$ (solid lines) and the Cooper-pair amplitude F_{k_f} (dashed lines) at the Fermi surface, after a sudden quench of the interaction from an initial value $U_0 = -3$ to $U = U_0 + \Delta U$. For weak excitations ΔU, the order parameter and F_{k_f} oscillate with a small amplitude, while both decay to zero for large ΔU (e.g., dark red lines). In general, F_{k_f} decays much slower than ϕ, even at relatively large interactions *and* excitations strong enough to melt the gap (see, e.g., the bold curve for $U = -0.6$). Hence there is a large time window where the vanishing of the order parameter ϕ is mainly due to dephasing, in spite of electron-electron scattering. This behavior can be unraveled by the noise correlation measurement. As the condensate of Cooper pairs is formed by electrons with opposite momentum p and $-p$, it is natural to measure the correlations $\Delta I_p \equiv \frac{1}{2}\sum_{\sigma,\sigma'} \Delta I_{p\sigma,-p\sigma'}$. For the BCS Hamiltonian one could use Wick's theorem to decouple the two-point function (2). The only nonvanishing contribution to the connected Green's function $G(1,2,2',1') - G(1,1')G(2,2')$ which enters the fluctuations ΔI_p is therefore related to an anomalous Green's function $\bar{G}_p(t,t') = \langle T_{\bar{t}}[c^\dagger_{p\uparrow}(t') c^\dagger_{-p\downarrow}(t)]\rangle$ [cf. Eqs. (4) and (3)],

$$\Delta I_p = \left| \int dt' dt'' S(t') S(t'') \bar{G}_p(t', t'') e^{i(E_p - \Omega)(t' + t'')} \right|^2, \quad (8)$$

where we set $M^{\sigma_1,\sigma}_{k,p} = \delta_{k\sigma_1,p\sigma}$ as explained above. As long as the system is initially deeply in the symmetry broken phase,

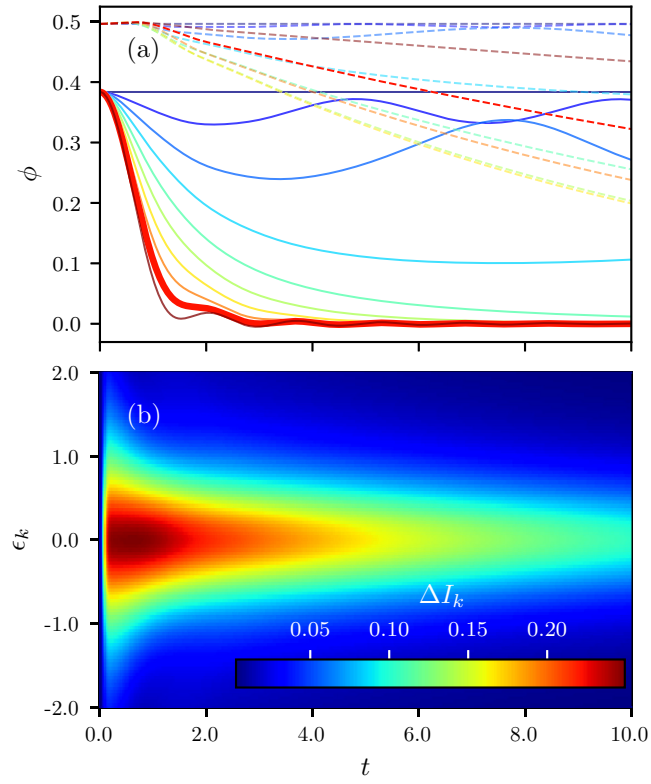

FIG. 1. (a) Order parameter ϕ (solid) and pairing correlations F_{k_f} (dashed) at the Fermi surface ($\epsilon_k = 0$) after an interaction quench with $\Delta U = 0.0, 0.3, \ldots, 2.7$ (top to bottom). The bold line corresponds to $\Delta U = 2.4$. (b) Numerical simulation of the noise correlation measurement for $\Delta U = 2.4$: $\Delta I_k(t)$, as obtained from Eq. (8) with a short pulse $S(\tau) = \sqrt{100/\pi} e^{-100(\tau - t)^2}$ centered around time t.

these anomalous terms capture the leading contribution to the two-particle Green's function even beyond mean-field theory (apart from vertex corrections). We therefore simply evaluate Eq. (8) using the DMFT solution. The simulated ARPES noise correlations, shown in Fig. 1(b), directly reveal the presence of Cooper-pair correlations beyond the vanishing of ϕ. A complementary tr-ARPES can detect the vanishing of ϕ by the closing of the spectral gap, so that the dephasing of the superconducting state can be identified. Vertex corrections to Eq. (8) would complicate a quantitative prediction of the value of ΔI_k, but the very different timescales for the two- and one-particle dynamics should remain a clear signature for experiment.

In the quench protocol, a strong excitation of the system simultaneously implies weak final interactions U. To simulate a strong impulsive excitation at large U, we perform a short pulse-shaped ramp of the interaction of duration τ, $U(t) = U_0 + \Delta U/2\theta(\tau - t)[1 + \cos(\pi t/\tau)]$. Figure 2(a) shows the resulting $\phi(t)$ (solid lines) and F_{k_f}. The relaxation dynamics is analyzed in a regime of relatively large $U = -3$, which is close to the maximum of the transition temperature $T_c(U)$ in the phase diagram, corresponding to the crossover into the strong-coupling regime of a BEC of preformed pairs. Similar to Fig. 1(a), amplitude mode oscillations or a melting of the gap are observed depending on the excitation ΔU, but

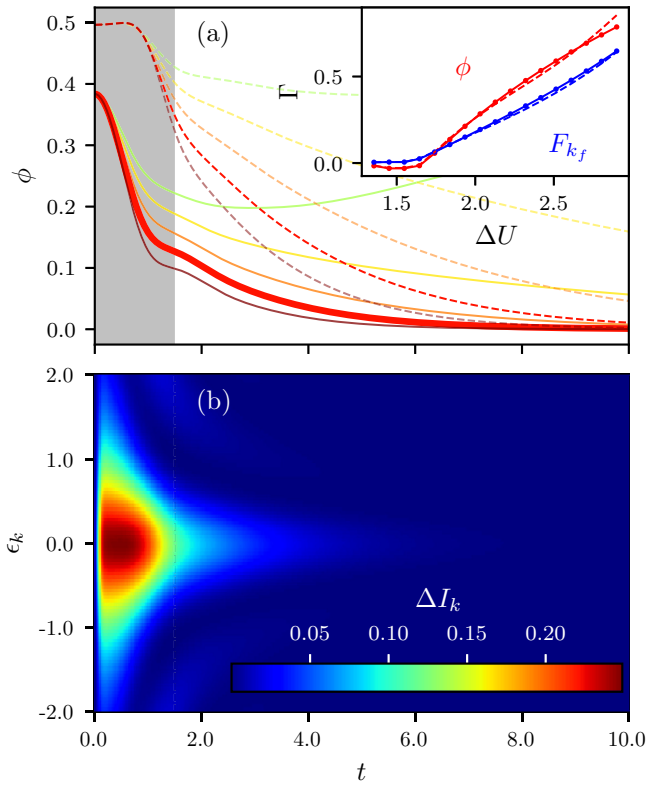

FIG. 2. (a) Order parameter ϕ (solid lines) and Cooper-pair correlations F_{k_f} (dashed lines) for the ramp protocol with different excitation densities $\Delta U = 1.5, 1.8, \ldots, 2.7$ (from top to bottom). The bold line shows $\Delta U = 2.4$. The shaded area highlights ramp duration period. Inset: Decay rate Γ obtained by an exponential fit to $\phi(t)$ (solid red), the momentum-averaged noise $\sum_k \sqrt{\Delta I_k(t)}$ (dashed red), F_{k_f} (solid, blue), and $\sqrt{\Delta I_{k_F}(t)}$ (dashed blue) against ΔU. (b) Numerical simulation of the noise correlation measurement $\Delta I_k(t)$ for energies around the Fermi edge for $\Delta U = 2.4$.

the larger electron-electron scattering now leads to a rapid relaxation of both the order parameter ϕ and F_{k_f}. The decay rates Γ_ϕ and Γ_F of ϕ and of F_{k_f} are of the same order, as shown by the solid lines in the inset of Fig. 2(a). (Both Γ_ϕ and Γ_F show a slowdown at the threshold $\Delta U \approx 1.6$ for the melting of the order.) The noise correlations [Fig. 2(b)] allow one to probe the dynamics of these quantities. In particular, by fitting an exponential decay $\exp(-\Gamma t)$ to the simulated data for $\sqrt{\Delta I_k(t)}$ and the momentum average $\sum_k \sqrt{\Delta I_k(t)}$, one can closely recover the corresponding rates Γ_ϕ and Γ_F (inset). In the present case, pairing interactions and scattering are controlled by the same microscopic interaction U, so that the melting happens on timescales still larger than $\hbar/\Delta$, which could be resolved in tr-ARPES. In general, however, there is no fundamental limitation for how fast ϕ can be quenched to zero, and the noise correlation measurement, which is independent of the spectral information, grants access to the pair correlations on timescales beyond the energy-time uncertainty limitations of tr-ARPES.

In conclusion, we have proposed to use the angular correlations in ARPES to characterize time-dependent two-particle correlations in the solid. The latter can be expected to dominate nonequilibrium states, but are hard to measure with other techniques. Exemplarily, we showed that the dephasing of the individual order parameter fluctuations can dominate the fast decay of superconductivity. Beyond this example, the noise correlation measurement could be used to probe transient charge-density-wave fluctuations (with correlations between momenta that differ by the nesting vector), excitonic correlations, or provide a different view on ultrafast dynamics of magnetic order [18], and possibly help to reveal fundamental phenomena such as a nonthermal criticality in solids [42,43]. These possibilities will be explored in future studies. Furthermore, there has been a considerable recent advance in the theoretical description of collective fluctuations in strongly correlated materials in equilibrium [44], so that more precise experimental measures for the two-particle Green's function are needed, even though fully irreducible two-particle quantities are hard to obtain with the current computational means. Equation (4) shows that even *dynamical* time- and energy-dependent two-particle quantities can be extracted from the noise correlation measurement.

In general, we conclude that the measurement of noise correlations in ARPES, though technically challenging, may give unique access to two-particle correlations in solids, which provides information that is indispensable to characterize the spatiotemporal evolution of nonequilibrium states.

We thank U. Bovensiepen and D. Fausti for useful discussions. We acknowledge the financial support from the DFG Project 310335100, and the ERC Starting Grant No. 716648.

[1] C. Giannetti, M. Capone, D. Fausti, M. Fabrizio, F. Parmigiani, and D. Mihailovic, Adv. Phys. **65**, 58 (2016).
[2] C. L. Smallwood, J. P. Hinton, C. Jozwiak, W. Zhang, J. D. Koralek, H. Eisaki, D.-H. Lee, J. Orenstein, and A. Lanzara, Science **336**, 1137 (2012).
[3] J. D. Rameau, S. Freutel, A. F. Kemper, M. A. Sentef, J. K. Freericks, I. Avigo, M. Ligges, L. Rettig, Y. Yoshida, H. Eisaki, J. Schneeloch, R. D. Zhong, Z. J. Xu, G. D. Gu, P. D. Johnson, and U. Bovensiepen, Nat. Commun. **7**, 13761 (2016).
[4] F. Schmitt, P. S. Kirchmann, U. Bovensiepen, R. G. Moore, L. Rettig, M. Krenz, J.-H. Chu, N. Ru, L. Perfetti, D. H. Lu, M. Wolf, I. R. Fisher, and Z.-X. Shen, Science **321**, 1649 (2008).
[5] T. Rohwer, S. Hellmann, M. Wiesenmayer, C. Sohrt, A. Stange, B. Slomski, A. Carr, Y. Liu, L. M. Avila, M. Kalläne, S. Mathias, L. Kipp, K. Rossnagel, and M. Bauer, Nature (London) **471**, 490 (2011).
[6] S. Mor, M. Herzog, D. Golež, P. Werner, M. Eckstein, N. Katayama, M. Nohara, H. Takagi, T. Mizokawa, C. Monney, and J. Stähler, Phys. Rev. Lett. **119**, 086401 (2017).
[7] L. Perfetti, P. A. Loukakos, M. Lisowski, U. Bovensiepen, H. Berger, S. Biermann, P. S. Cornaglia, A. Georges, and M. Wolf, Phys. Rev. Lett. **97**, 067402 (2006).
[8] D. Wegkamp, M. Herzog, L. Xian, M. Gatti, P. Cudazzo, C. L. McGahan, R. E. Marvel, R. F. Haglund, A. Rubio,

M. Wolf, and J. Stähler, Phys. Rev. Lett. **113**, 216401 (2014).
[9] M. Ligges, I. Avigo, D. Golež, H. U. R. Strand, Y. Beyazit, K. Hanff, F. Diekmann, L. Stojchevska, M. Kalläne, P. Zhou, K. Rossnagel, M. Eckstein, P. Werner, and U. Bovensiepen, Phys. Rev. Lett. **120**, 166401 (2018).
[10] Y. H. Wang, H. Steinberg, P. Jarillo-Herrero, and N. Gedik, Science **342**, 453 (2013).
[11] In this case, a subtle deconvolution of the spectrum from the probe envelope in time and frequency, or a suitable pulse shaping of the probe pulse may be needed to extract the relevant dynamical information.
[12] H. Krull, D. Manske, G. S. Uhrig, and A. P. Schnyder, Phys. Rev. B **90**, 014515 (2014).
[13] R. A. Barankov and L. S. Levitov, Phys. Rev. Lett. **96**, 230403 (2006).
[14] A. F. Kemper, M. A. Sentef, B. Moritz, J. K. Freericks, and T. P. Devereaux, Phys. Rev. B **92**, 224517 (2015).
[15] F. Peronaci, M. Schiró, and M. Capone, Phys. Rev. Lett. **115**, 257001 (2015).
[16] R. Matsunaga, Y. I. Hamada, K. Makise, Y. Uzawa, H. Terai, Z. Wang, and R. Shimano, Phys. Rev. Lett. **111**, 057002 (2013).
[17] S. Wall, S. Yang, L. Vidas, M. Chollet, J. M. Glownia, M. Kozina, T. Katayama, T. Henighan, M. Jiang, T. A. Miller, D. A. Reis, L. A. Boatner, O. Delaire, and M. Trigo, Science **362**, 572 (2018).
[18] S. Eich, M. Plötzing, M. Rollinger, S. Emmerich, R. Adam, C. Chen, H. C. Kapteyn, M. M. Murnane, L. Plucinski, D. Steil, B. Stadtmüller, M. Cinchetti, M. Aeschlimann, C. M. Schneider, and S. Mathias, Sci. Adv. **3**, e1602094 (2017).
[19] J. Bauer, M. Babadi, and E. Demler, Phys. Rev. B **92**, 024305 (2015).
[20] Y. Lemonik and A. Mitra, Phys. Rev. B **96**, 104506 (2017).
[21] N. Dasari and M. Eckstein, Phys. Rev. B **98**, 235149 (2018).
[22] K. Ido, T. Ohgoe, and M. Imada, Sci. Adv. **3**, e1700718 (2017).
[23] E. Altman, E. Demler, and M. D. Lukin, Phys. Rev. A **70**, 013603 (2004).
[24] I. Bloch, J. Dalibard, and W. Zwerger, Rev. Mod. Phys. **80**, 885 (2008).
[25] M. Esposito, K. Titimbo, K. Zimmermann, F. Giusti, F. Randi, D. Boschetto, F. Parmigiani, R. Floreanini, F. Benatti, and D. Fausti, Nat. Commun. **6**, 10249 (2015).
[26] F. Randi, M. Esposito, F. Giusti, O. Misochko, F. Parmigiani, D. Fausti, and M. Eckstein, Phys. Rev. Lett. **119**, 187403 (2017).
[27] F. O. Schumann, C. Winkler, and J. Kirschner, Phys. Status Solidi B **246**, 1483 (2009).
[28] Y. Pavlyukh, M. Schüler, and J. Berakdar, Phys. Rev. B **91**, 155116 (2015).
[29] A. Trützschler, M. Huth, C.-T. Chiang, R. Kamrla, F. O. Schumann, J. Kirschner, and W. Widdra, Phys. Rev. Lett. **118**, 136401 (2017).
[30] M. Sakaue, J. Phys.: Condens. Matter **17**, S245 (2005).
[31] C. Timm and K. H. Bennemann, J. Phys.: Condens. Matter **16**, 661 (2004).
[32] H. Ueba and B. Gumhalter, Prog. Surf. Sci. **82**, 193 (2007).
[33] J. K. Freericks, H. R. Krishnamurthy, and T. Pruschke, Phys. Rev. Lett. **102**, 136401 (2009).
[34] M. Eckstein and M. Kollar, Phys. Rev. B **78**, 245113 (2008).
[35] A. F. Kemper, M. A. Sentef, B. Moritz, T. P. Devereaux, and J. K. Freericks, Ann. Phys. **529**, 1600235 (2017).
[36] See Supplemental Material at http://link.aps.org/supplemental/10.1103/PhysRevB.99.241111 for the details of the derivation of the integrals $I^{(1)}_{p\sigma}$ and $I^{(2)}_{p\sigma,p'\sigma'}$.
[37] F. Randi, D. Fausti, and M. Eckstein, Phys. Rev. B **95**, 115132 (2017).
[38] P. W. Anderson, Phys. Rev. **112**, 1900 (1958).
[39] E. A. Yuzbashyan and M. Dzero, Phys. Rev. Lett. **96**, 230404 (2006).
[40] E. A. Yuzbashyan, O. Tsyplyatyev, and B. L. Altshuler, Phys. Rev. Lett. **96**, 097005 (2006).
[41] H. Aoki, N. Tsuji, M. Eckstein, M. Kollar, T. Oka, and P. Werner, Rev. Mod. Phys. **86**, 779 (2014).
[42] J. Berges, A. Rothkopf, and J. Schmidt, Phys. Rev. Lett. **101**, 041603 (2008).
[43] N. Tsuji, M. Eckstein, and P. Werner, Phys. Rev. Lett. **110**, 136404 (2013).
[44] G. Rohringer, H. Hafermann, A. Toschi, A. A. Katanin, A. E. Antipov, M. I. Katsnelson, A. I. Lichtenstein, A. N. Rubtsov, and K. Held, Rev. Mod. Phys. **90**, 025003 (2018).